Journal of Virology

Virology | Full-Length Text

# NLRP1 restricts porcine deltacoronavirus infection via IL-11 inhibiting the phosphorylation of the ERK signaling pathway

**Haojie He,[1] Yongfeng Li,[1] Yunyan Chen,[1] Jianfei Chen,[1] Zhongyuan Li,[1] Liang Li,[1] Da Shi,[1] Xin Zhang,[1] Hongyan Shi,[1] Mei Xue,[1] Li Feng[1]**

**AUTHOR AFFILIATION** See affiliation list on p. 19.

**ABSTRACT** Continuously emerging highly pathogenic coronaviruses remain a major threat to human and animal health. Porcine deltacoronavirus (PDCoV) is a newly emerging enterotropic swine coronavirus that causes large-scale outbreaks of severe diarrhea disease in piglets. Unlike other porcine coronaviruses, PDCoV has a wide range of species tissue tropism, including primary human cells, which poses a significant risk of cross-species transmission. Nucleotide-binding oligomerization domain-like receptor (NLR) family pyrin domain-containing 1 (NLRP1) has a key role in linking host innate immunity to microbes and the regulation of inflammatory pathways. We now report a role for NLRP1 in the control of PDCoV infection. Overexpression of NLRP1 remarkably suppressed PDCoV infection, whereas knockout of NLRP1 led to a significant increase in PDCoV replication. A mechanistic study revealed that NLRP1 suppressed PDCoV replication in cells by upregulating IL-11 expression, which in turn inhibited the phosphorylation of the ERK signaling pathway. Furthermore, the ERK phosphorylation inhibitor U0126 effectively hindered PDCoV replication in pigs. Together, our results demonstrated that NLRP1 exerted an anti-PDCoV effect by IL-11-mediated inhibition of the phosphorylation of the ERK signaling pathway, providing a novel antiviral signal axis of NLRP1-IL-11-ERK. This study expands our understanding of the regulatory network of NLRP1 in the host defense against virus infection and provides a new insight into the treatment of coronaviruses and the development of corresponding drugs.

**IMPORTANCE** Coronavirus, which mainly infects gastrointestinal and respiratory epithelial cells *in vivo*, poses a huge threat to both humans and animals. Although porcine deltacoronavirus (PDCoV) is known to primarily cause fatal diarrhea in piglets, reports detected in plasma samples from Haitian children emphasize the potential risk of animal-to-human spillover. Finding effective therapeutics against coronaviruses is crucial for controlling viral infection. Nucleotide-binding oligomerization-like receptor (NLR) family pyrin domain-containing 1 (NLRP1), a key regulatory factor in the innate immune system, is highly expressed in epithelial cells and associated with the pathogenesis of viruses. We demonstrate here that NLRP1 inhibits the infection of the intestinal coronavirus PDCoV through IL-11-mediated phosphorylation inhibition of the ERK signaling pathway. Furthermore, the ERK phosphorylation inhibitor can control the infection of PDCoV in pigs. Our study emphasizes the importance of NLRP1 as an immune regulatory factor and may open up new avenues for the treatment of coronavirus infection.

**KEYWORDS** porcine deltacoronavirus, nucleotide-binding oligomerization domain-like receptor family pyrin domain-containing 1, interleukin-11, ERK signaling, anti-coronavirus

**Editor** Tom Gallagher, Loyola University Chicago - Health Sciences Campus, Maywood, Illinois, USA

Address correspondence to Mei Xue, xuemei_23@126.com, or Li Feng, fengli@caas.cn.

Haojie He and Yongfeng Li contributed equally to this article. Author order was determined both alphabetically and in order of increasing seniority.

The authors declare no conflict of interest.

See the funding table on p. 19.

**Received** 20 December 2023
**Accepted** 8 February 2024
**Published** 27 February 2024

Porcine deltacoronavirus (PDCoV) is an enveloped, single-stranded positive-sense RNA virus with a genome length of approximately 25.4 kb, belonging to the order *Nidovirales*, family *Coronaviridae*, subfamily *Orthocoronavirinae*, and genus *Deltacoronavirus*. It was initially reported in wild Asian leopard cats (*Prionailurus bengalensis*) and Chinese ferret badgers (*Melogalemoschata*) in 2007, and subsequently identified in various avian species and domestic pigs (1–3). In 2012, Woo et al. (3) reported the first PDCoV strain HKU15 in Hong Kong, confirming the existence of deltacoronaviruses in mammals. In early 2014, PDCoV was first associated with cases of porcine diarrhea in Ohio, Iowa, and Illinois in the United States (4, 5). Subsequent research revealed that PDCoV has spread globally, primarily affecting Asian countries and North American countries (6). Pigs of all age groups are susceptible to PDCoV infection, with piglets being the most vulnerable and experiencing high mortality rates. Infected piglets mainly exhibit acute watery diarrhea, vomiting, and dehydration, accompanied by depression, lethargy, and reduced appetite, causing serious harm to the swine industry (7, 8). In recent years, there have been numerous reports on the interspecies transmission of PDCoV. Current research has indicated that PDCoV can infect species beyond pigs, including calves, chickens, turkeys, and mice (9–12). Moreover, in 2021, PDCoV was even detected in plasma samples from children in Haiti, further highlighting its potential for interspecies transmission (13). Consequently, the need for an effective drug against PDCoV is urgent.

Nucleotide-binding oligomerization domain-like receptor family pyrin domain-containing 1 (NLRP1) is a pivotal member of the NLR protein family, profoundly involved in regulating innate immunity and inflammatory responses (14). It plays a crucial role in the host defense against infections by recognizing various pathogens, including bacteria and viruses (15–19). Upon detection of pathogen-associated molecular patterns (PAMPs) or danger-associated molecular patterns, NLRP1 assembles an inflammasome complex with the adaptor protein apoptosis-associated speck-like protein containing a CARD (ASC) and caspase-1 (20). This assembly leads to the cleavage of pro-inflammatory cytokines, such as pro-IL-1β and pro-IL-18, into their active forms. Consequently, the released active IL-1β and IL-18 trigger a potent inflammatory response, contributing to infection clearance and tissue repair processes. While direct involvement of the NLRP1 protein in the antiviral process lacks evidence, our previous research has shown that NLRP1 itself can act as an interferon-stimulating gene (ISG) to combat the infection of transmissible gastroenteritis virus (TGEV) (21). This finding suggests that NLRP1 possesses the potential to resist virus infection.

Interleukin-11 (IL-11) is a versatile cytokine belonging to the IL-6 family (22). It mediates its effects through the IL-11 receptor, which exists as a heterodimer consisting of IL-11 receptor alpha (IL-11Rα) and the common cytokine receptor subunit, gp130 (23). IL-11 plays a crucial role in modulating diverse biological processes, including hematopoiesis, inflammation, tissue repair, and immunity against viral infections (23–25). IL-11 exhibits potent abilities in promoting intestinal cell proliferation and inhibiting apoptosis, playing a crucial protective role against various injuries to intestinal epithelial cells (26–28). These cells serve as target cells for porcine enteric coronaviruses. Studies have revealed that during porcine epidemic diarrhea virus (PEDV) infection, IL-11 activates the IL-11/STAT3 signaling pathway to impede PEDV-induced cell apoptosis, thereby suppressing viral infection (25). Moreover, several signaling pathways, such as the mitogen-activated protein kinase/extracellular signal-regulated kinase (MAPK/ERK) and phosphatidylinositol 3-kinase (PI3K)/AKT, have also been implicated in the regulatory pathway of IL-11 (23).

Our study showed that NLRP1 suppressed PDCoV replication in cells by upregulating IL-11 expression, which in turn inhibited the phosphorylation of the ERK signaling pathway. Furthermore, the ERK phosphorylation inhibitor U0126 effectively hindered PDCoV replication in pigs. Our findings establish a novel link between NLRP1 and IL-11, providing new insights into NLR-guided signal pathway and offering a promising therapeutic strategy for coronavirus infections.

## RESULTS

### NLRP1 inhibits the replication of PDCoV

We previously showed that NLRP1 has antiviral capabilities against TGEV infection, but it is still unclear whether NLRP1 can antagonize other coronaviruses (21). To investigate the impact of NLRP1 on PDCoV replication, we initially constructed a eukaryotic expression plasmid, Flag-NLRP1, tagged with a Flag epitope. Subsequently, immortal pig intestinal-2I (IPI-2I) cells were transfected with the plasmid and infected with PDCoV at an MOI of 0.1 after 24 h of transfection. Following a 24-h infection period, cell samples were collected, and total RNA was extracted. The results from real-time quantitative PCR (RT-qPCR), as shown in Fig. 1A and B, revealed a significant reduction of approximately 91.2% in PDCoV replication levels within the NLRP1-transfected IPI-2I cells compared to

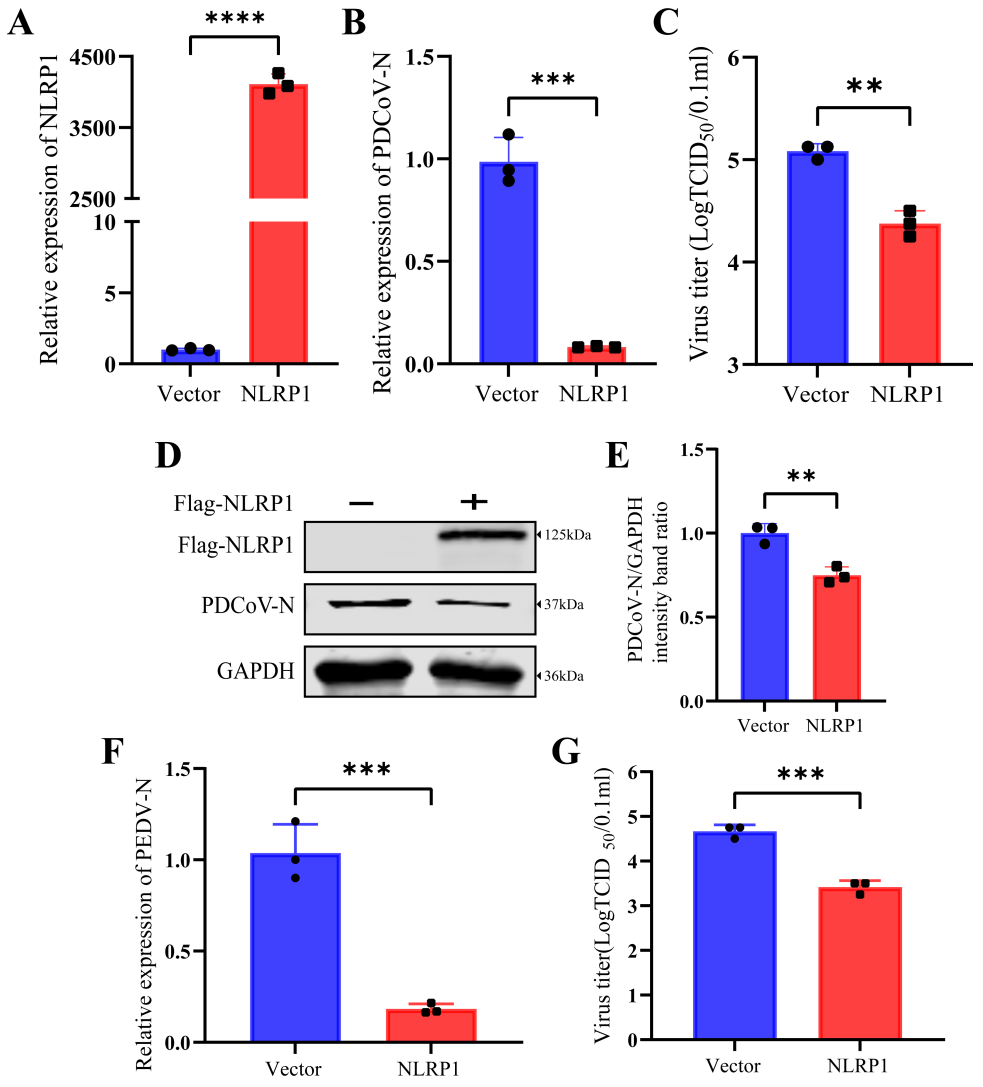


**FIG 1** pNLRP1 inhibits the replication of PDCoV. IPI-2I cells were transfected with Flag-tagged NLRP1 (0 or 1 µg) for 24 h, followed by infection with PDCoV at an MOI of 0.1 for 24 h. (A) The overexpression of NLRP1 was verified by RT-qPCR. (B) The relative expression of PDCoV was determined by RT-qPCR. (C) The PDCoV $TCID_{50}$ in the supernatants was titrated on swine testis cells. (D) The protein expression of NLRP1 and PDCoV-N was detected by Western blotting. (E) The relative intensities of PDCoV-N were normalized to glyceraldehyde-3-phosphate dehydrogenase (GAPDH). (F) IPI-2I cells were transfected with Flag-tagged NLRP1 (0 or 1 µg) for 24 h, followed by infection with PEDV at an MOI of 1 for 24 h. The relative expression of PEDV was determined by RT-qPCR. (G) The PEDV $TCID_{50}$ in the supernatants was titrated on Vero-E6 cells. The means and SD of the results from three independent experiments are shown. $^{**}P < 0.01$; $^{***}P < 0.001$; and $^{****}P < 0.0001$.

the control group. In addition, cell culture supernatants were collected to determine the viral titers, and the results showed that the viral titers were substantially reduced in NLRP1-transfected cells (Fig. 1C). Subsequently, we collected cell samples under the same conditions for further validation by Western blotting. The results, presented in Fig. 1D and E, demonstrated a remarkable decrease in the expression level of PDCoV-N protein within the NLRP1-transfected group. Additionally, overexpression of NLRP1 also inhibits the replication of PEDV (Fig. 1F and G), indicating that NLRP1 plays an important role in resisting coronavirus replication.

## Knockdown or knockout of NLRP1 enhances PDCoV replication

To further confirm the inhibitory effect of NLRP1 on PDCoV replication, we designed two small interfering RNAs (siRNAs) specifically targeting NLRP1, named siNLRP1#1 and siNLRP1#2. Initially, we demonstrated the significant knockdown effects of siRNAs by Western blotting and RT-qPCR (Fig. 2A, D, and E). Subsequently, siNLRP1#1, siNLRP1#2, and a negative control siRNA (NC) were simultaneously transfected into IPI-2I cells for 24 h, and the cells were infected with PDCoV at an MOI of 0.1. The intracellular relative NLRP1 expression and viral loads were tested by Western blotting and RT-qPCR at 24 h post-infection (hpi). As shown in Fig. 2A and B, the mRNA levels of endogenous NLRP1 in IPI-2I cells decreased by approximately 38% and 56%, respectively, while the replication level of PDCoV increased significantly compared with the negative control. Furthermore, the cell culture supernatants were collected, and the viral titers were determined by assessing the 50% tissue culture infective dose ($TCID_{50}$). As indicated in Fig. 2C, the viral titers in NLRP1-overexpressed cells increased by approximately 10-fold compared with the negative control. Corresponding to the mRNA levels, the tendency of siNLRP1#1 or siNLRP1#2 to promote PDCoV propagation was observed by Western blotting (Fig. 2D through F). In addition, pNLRP1 (porcine NLRP1) knockout ($NLRP1^{-/-}$) IPI-2I cells, which we established in a previous report, were infected with PDCoV at an MOI of 0.1 and then harvested to test viral loads by RT-qPCR, Western blotting, and viral titers by $TCID_{50}$. As expected, PDCoV replication was increased significantly in $NLRP1^{-/-}$IPI-2I cells compared with WT IPI-2I cells (Fig. 2G through J). Taken together, these results supported that the NLRP1 plays a role in counteracting PDCoV replication.

## NLRP1 does not rely on the IFN pathway to inhibit PDCoV replication

It has been reported that NLRP6 can bind to viral RNA through the RNA helicase Dhx15 and interact with mitochondrial antiviral signaling protein (MAVS), inducing the upregulation of type I and III interferons (IFNs) and ISGs (29). This mechanism helps to regulate the antiviral response within the intestinal tract. Since both NLRP1 and NLRP6 belong to the NLR family, we initially speculated that IFNs may play a role in NLRP1-mediated antiviral processes. As shown in Fig. 3A and B, the mRNA and protein levels of IFN-β in PDCoV-infected IPI-2I cells displayed a dose-dependent decrease after 24 hpi, consistent with the previous report (30). However, when NLRP1 was overexpressed in IPI-2I cells and subsequently infected with PDCoV, the mRNA and protein levels of IFN-β showed no significant difference compared to the mock group (Fig. 3C and D). Therefore, these results suggested that IFN-I does not play a crucial role in the NLRP1-mediated antiviral process.

To further explore the mechanism that may be associated with the antiviral effect of NLRP1, we examined the transcript levels of some relevant cytokines in the inflammatory pathway in cell samples overexpressing NLRP1 and infected with PDCoV. As shown in Fig. 3E, compared to IL-18 and IL-1β, which play roles in the classical inflammatory pathway, the transcription level of IL-11 was upregulated approximately 9.1-fold in these samples. To understand the relationship between human, pig, rat, and mouse IL-11 nucleotide sequences, we performed multiple sequence alignment, as shown in Fig. 3F, which revealed a high homology of 93% between pig and human IL-11 sequences. Subsequently, we used an ELISA kit specifically targeting human IL-11 to measure the secretion of IL-11 in the supernatant of two sets of samples: one with NLRP1 overexpression and

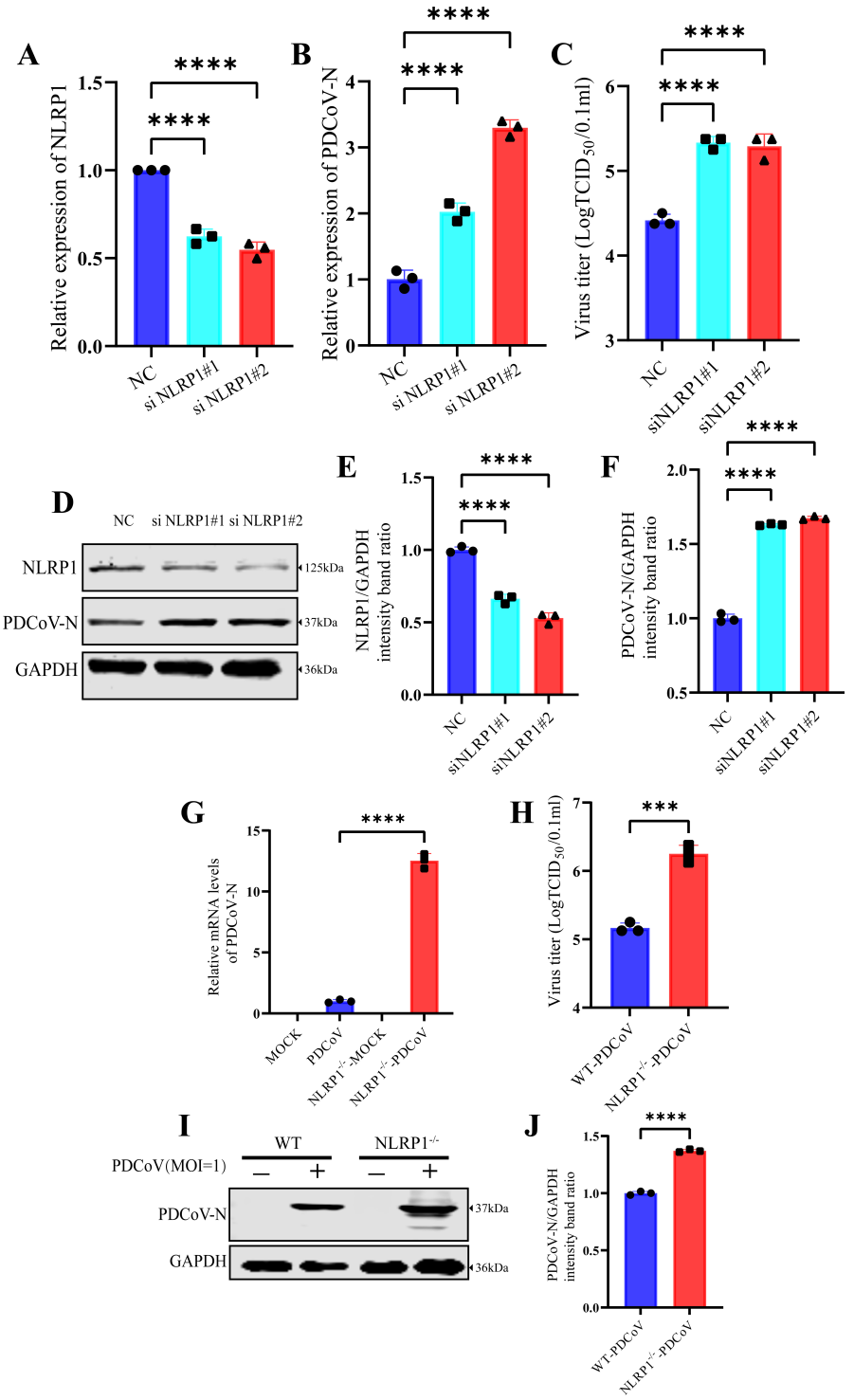


**FIG 2** Knockdown or knockout of NLRP1 enhances PDCoV replication. IPI-2I cells were transfected with siNLRP1#1, siNLRP1#2, or NC at 50 nM for 24 h and subsequently infected with PDCoV at an MOI of 0.1 for 24 h. (A and B) mRNA levels of NLRP1 and PDCoV-N in NLRP1 knockdown cells. (C) The PDCoV $TCID_{50}$ in the supernatants was titrated on swine testis (ST) cells. (D–F) Expression of NLRP1 and PDCoV-N was detected by Western blotting, and the relative intensities of NLRP1 and PDCoV-N were normalized to that of glyceraldehyde-3-phosphate dehydrogenase (GAPDH). (G and I) WT IPI-2I cells and $NLRP1^{-/-}$ IPI-2I cells were infected with PDCoV at an MOI of 0.1 for 24 h, and then the relative mRNA levels and protein levels of PDCoV-N were detected by RT-qPCR (G) and Western blotting (I). (H) The PDCoV $TCID_{50}$ in the supernatants of WT or $NLRP1^{-/-}$ IPI-2I cell was titrated on ST cells. (J) The relative intensity of PDCoV-N was normalized to that of GAPDH. The means and SD of the results from three independent experiments are shown. ***$P < 0.001$ and ****$P < 0.0001$.

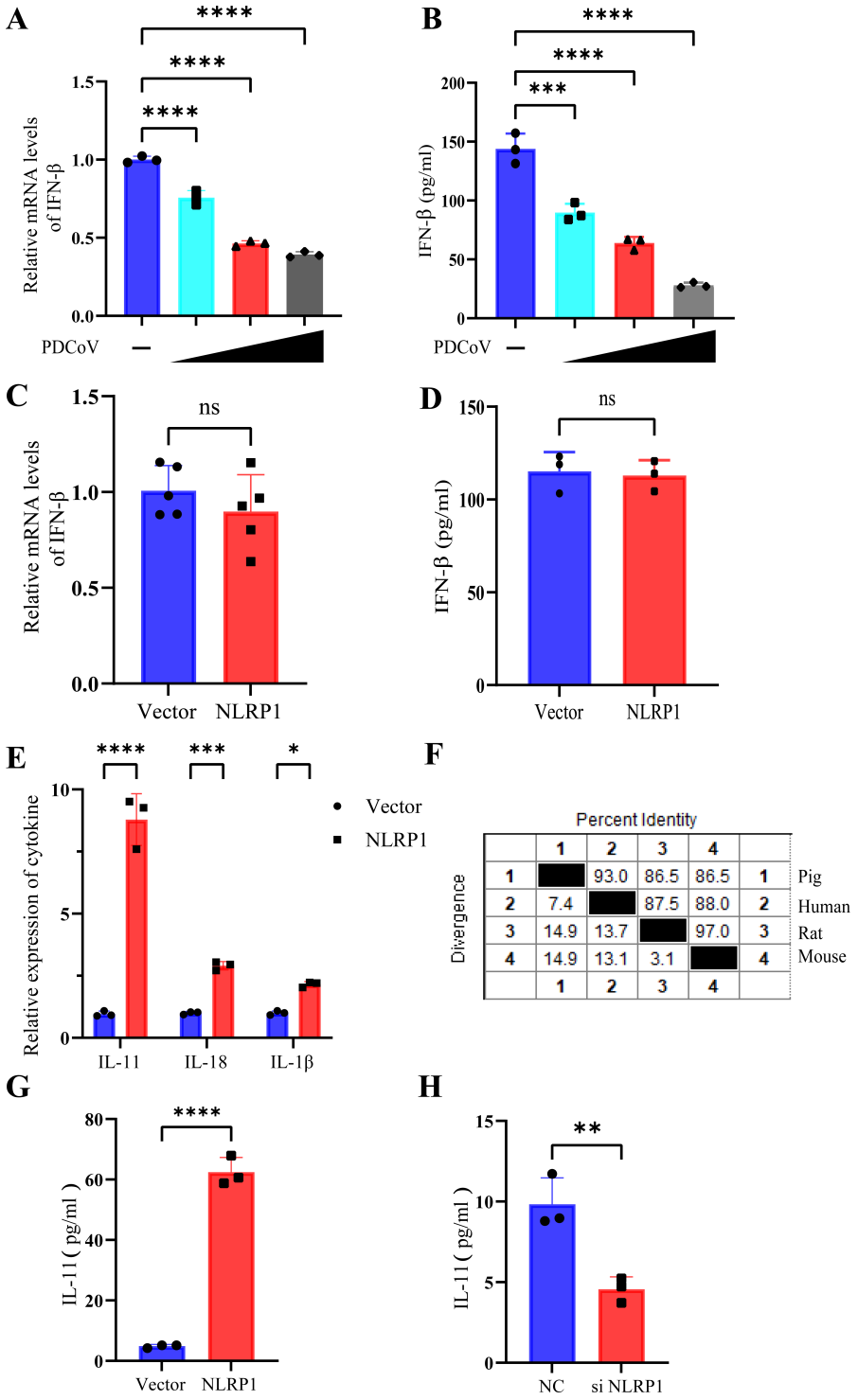


**FIG 3** NLRP1 does not rely on the IFN pathway to inhibit PDCoV replication. (A and B) The mRNA levels of IFN-β were detected by RT-qPCR (A) and the protein levels of IFN-β were detected by ELISA (B) in IPI-2I cells either mock infected or infected with PDCoV at MOI of 0.01, 0.1, and 1. (C–E) The mRNA expression of IFN-β (C) and cytokines (E) was measured by RT-qPCR, and the protein expression of IFN-β was measured by ELISA in NLRP1-overexpression cells. (F) Multiple sequence alignment between the pig, human, rat, and mouse. (G and H) Protein levels of IL-11 in the supernatant of NLRP1-overexpression cells (G) or NLRP1-knockdown cells (H) were analyzed by ELISA. The means and SD of the results from three independent experiments are shown. ns, no significant difference. *$P < 0.05$; **$P < 0.01$; ***$P < 0.001$; and ****$P < 0.0001$.

PDCoV infection, and the other with NLRP1 knockdown and PDCoV infection. The results in Fig. 3G and H demonstrated that NLRP1 overexpression significantly upregulated the expression of IL-11, while NLRP1 knockdown led to a significant decrease in IL-11 secretion. These findings indicated that NLRP1 may exert antiviral effects through IL-11.

## The treatment of IL-11 recombinant protein inhibits the replication of PDCoV

To further validate this hypothesis, we treated PDCoV-infected cells with various concentrations of exogenous IL-11 recombinant protein for 24 h. The results from RT-qPCR and Western blotting indicated that IL-11 treatment significantly suppressed PDCoV replication, with intracellular virus replication levels reduced by approximately 35.6%, 81.5%, and 98.8%, showing a dose-dependent manner (Fig. 4A through C). Subsequently, we treated IPI-2I cells infected with different MOI of PDCoV with 100 ng/mL of IL-11, and the results are shown in Fig. 4D through F. Compared with the mock group, the IL-11-treated group exhibited a substantial reduction in virus replication, and interestingly, the inhibitory effect of IL-11 was more pronounced in cells

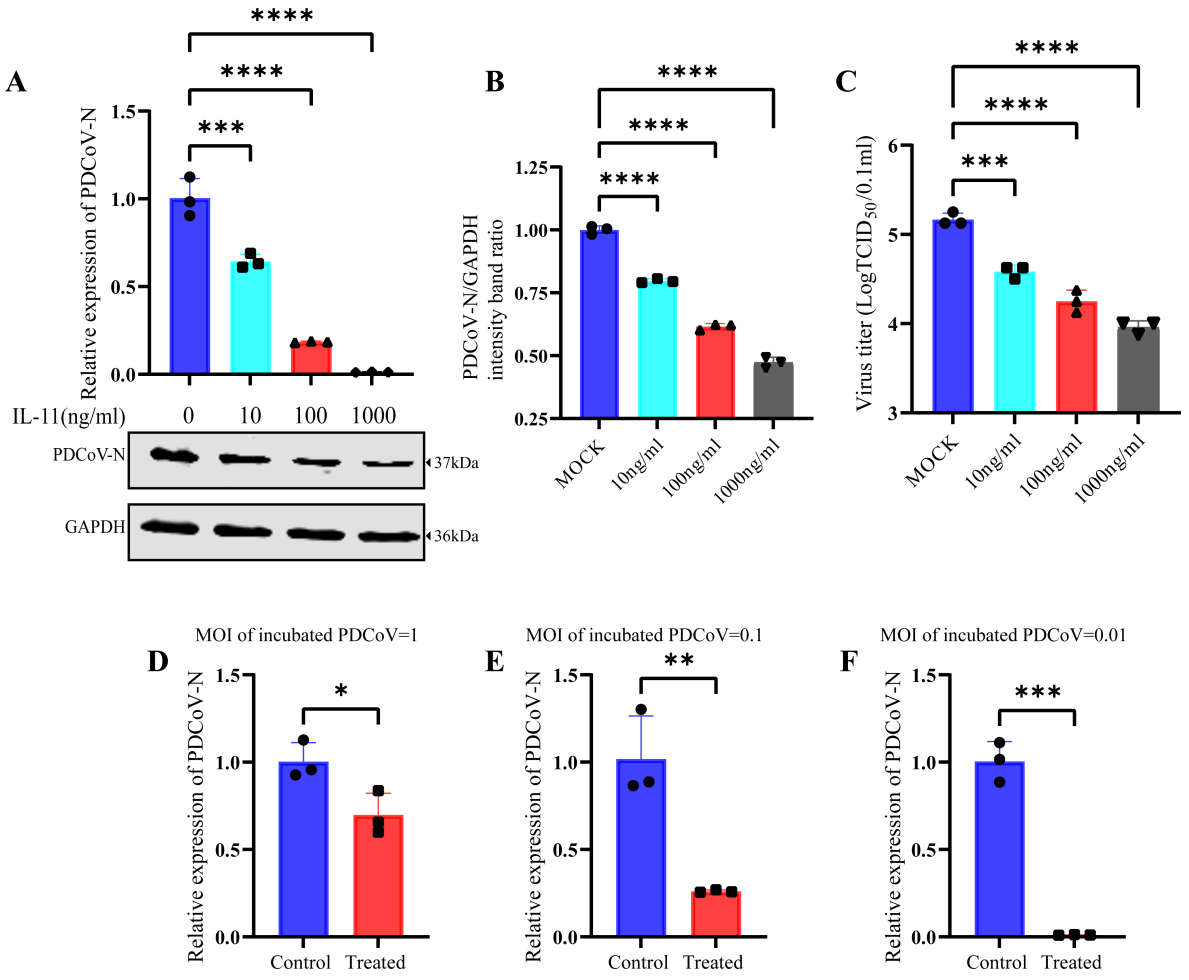


**FIG 4** The treatment of IL-11 recombinant protein inhibits the replication of PDCoV. After incubation with 0.1 MOI of PDCoV for 2 h at 37°C, IPI-2I cells were washed three times with phosphate-buffered saline (PBS) to remove unbound virus and then treated with different concentrations of IL-11 protein (0, 10, 100, or 1,000 ng/mL) for 24 h. (A) The relative viral copy number of PDCoV and the protein expression level of PDCoV-N were measured by RT-qPCR and Western blotting, respectively. (B) The relative intensity of PDCoV-N was normalized to that of glyceraldehyde-3-phosphate dehydrogenase (GAPDH). (C) The PDCoV $TCID_{50}$ in the supernatants of IPI-2I cells was titrated on swine testis cells. (D–F) The relative viral RNA copy number of PDCoV in IL-11-treated cells. After incubation with 0.01 (F), 0.1 (E), or 1 (D) MOI of PDCoV for 2 h at 37°C, IPI-2I cells were washed three times with PBS to remove unbound virus and then treated with 100 ng/mL of IL-11 protein for 24 h. The means and SD of the results from three independent experiments are shown. ns, no significant difference. *$P < 0.05$; **$P < 0.01$; ***$P < 0.001$; and ****$P < 0.0001$.

infected with the lower MOI. These results provided further support for our hypothesis that NLRP1 exerts its antiviral effect through the regulation of IL-11 expression.

### Knockdown of IL-11RA enhances PDCoV infection

During intercellular signal transduction, IL-11 forms a hexameric complex composed of IL-11, IL-11 receptor alpha (IL-11RA), and gp130 proteins in a 2:2:2 ratio (23). Theoretically, knocking down IL-11RA can effectively block IL-11 signaling and prevent its function. Therefore, to further explore the impact of IL-11 on PDCoV replication, we designed two siRNAs specifically targeting pig IL-11RA. Subsequently, IPI-2I cells were separately transfected with siIL-11RA#1, siIL-11RA#2, and NC, followed by infection with PDCoV at an MOI of 0.1 for 24 h. As shown in Fig. 5A, compared to the NC group, the mRNA levels of IL-11RA in cells transfected with siRNA were reduced by approximately 69% and 67%, respectively. The results demonstrated that after knocking down IL-11RA, PDCoV replication levels increased by approximately 8.33- and 8.29-fold (Fig. 5B), which is consistent with the result of virus titer (Fig. 5C). Furthermore, as depicted in Fig. 5D

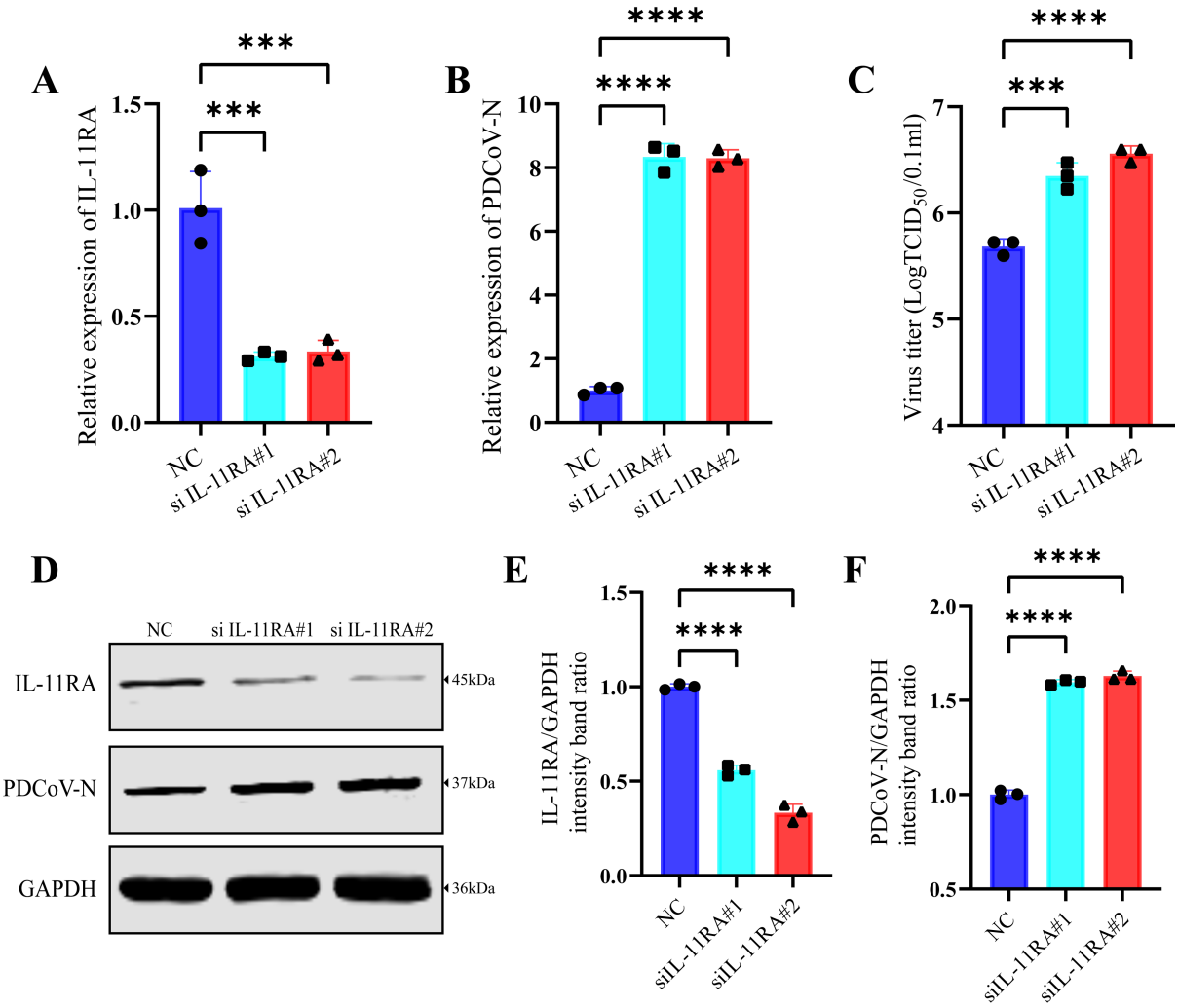


**FIG 5** Knockdown of IL-11RA enhances PDCoV infection. IPI-2I cells were transfected with IL-11RA#1, IL-11RA#2, or NC at 50 nM for 24 h and subsequently infected with PDCoV at an MOI of 0.1 for 24 h. (A and B) mRNA levels of IL-11RA and PDCoV-N in IL-11RA knockdown cells. (C) The PDCoV $TCID_{50}$ in the supernatants was titrated on swine testis cells. (D–F) Expression of IL-11RA and PDCoV-N was detected by Western blotting, and the relative intensities of NLRP1 and PDCoV-N were normalized to that of glyceraldehyde-3-phosphate dehydrogenase (GAPDH). The means and SD of the results from three independent experiments are shown. ***$P < 0.001$ and ****$P < 0.0001$.

through F, a notable upregulation in PDCoV replication was observed when IL-11RA protein expression was reduced by Western blotting. Collectively, these data confirmed that knocking down IL-11RA significantly promotes PDCoV replication.

### NLRP1 relies on the IL-11 pathway to inhibit PDCoV replication

To further verify whether NLRP1 exerts its antiviral effect through IL-11, we decided to compare the viral replication in cells overexpressing NLRP1 and infected with PDCoV with or without knocking down IL-11RA. To prepare the IL-11RA knockdown cell samples, we first transfected IPI-2I cells with 50 nM of siIL-11RA#2 or NC (control group). After 12 h, we transfected 1 µg of NLRP1 eukaryotic expression plasmid, and 24 h later, the cells were infected with PDCoV at an MOI of 0.1. Cell samples were collected at 24 hpi. As shown in Fig. 6A, 1C, and D, when IL-11RA was not knocked down, the overexpression of NLRP1 effectively suppressed PDCoV replication at both the protein and mRNA levels. However, after knocking down IL-11RA (Fig. 6B through D), the overexpression of NLRP1 failed to significantly inhibit PDCoV replication. These results indicated that when IL-11RA is knocked down, the pathway through which NLRP1 relies on IL-11 to exert its

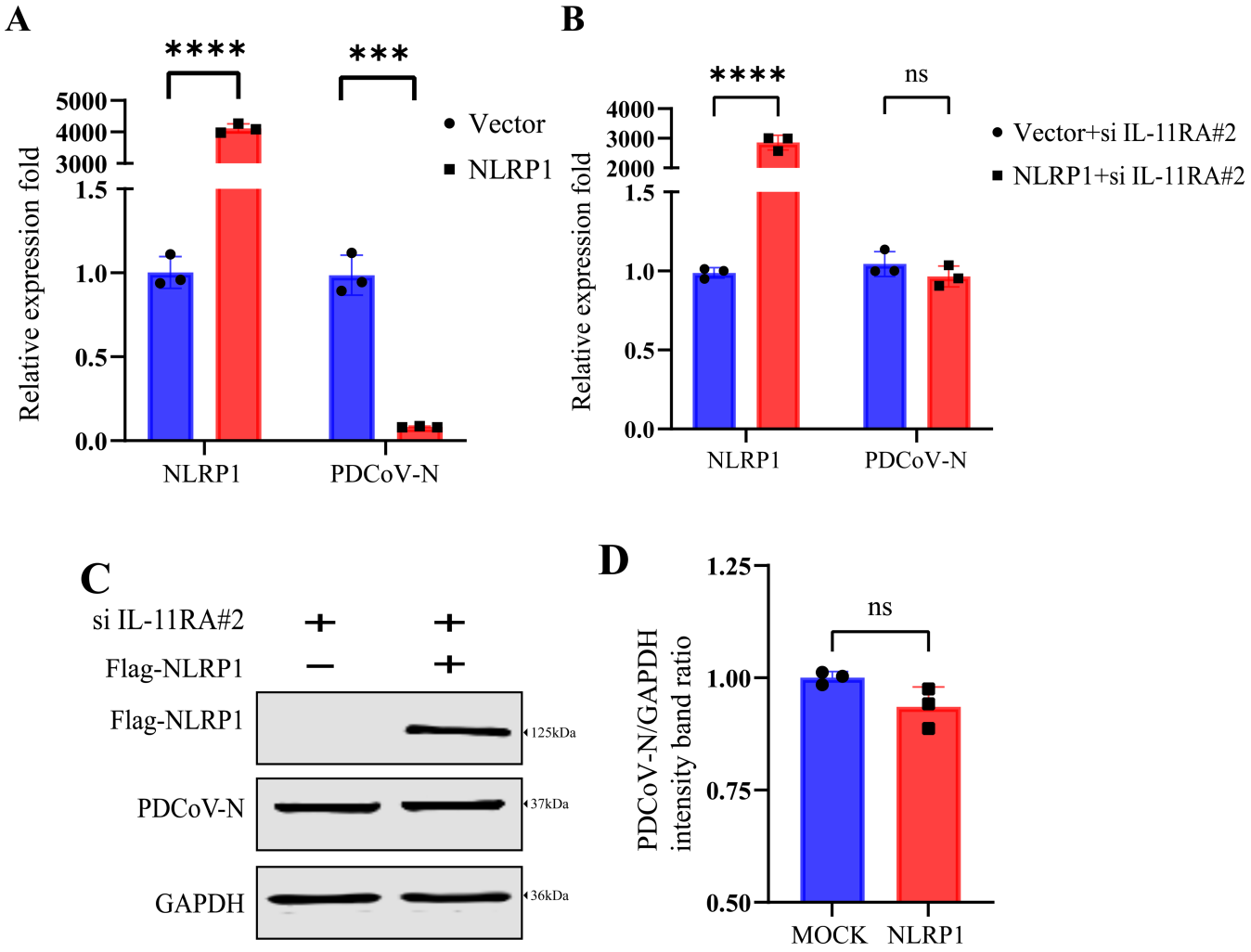


**FIG 6** NLRP1 relies on the IL-11 pathway to inhibit PDCoV replication. After transfection with 50 nM of siIL-11RA#2 or NC for 12 h, IPI-2I cells were transfected with 1 µg of Flag-tagged NLRP1 for 24 h and then infected with PDCoV at an MOI of 0.1 for 24 h. (A and B) The relative expression of NLRP1 and PDCoV-N in NC (A) or IL-11-knockdown cells (B). (C) The protein expression of PDCoV-N was detected by Western blotting. (D) The relative intensity of PDCoV-N was normalized to that of glyceraldehyde-3-phosphate dehydrogenase (GAPDH). The means and SD of the results from three independent experiments are shown. ns, no significant difference. ***$P < 0.001$ and ****$P < 0.0001$.

antiviral effect is blocked. In conclusion, NLRP1 depends on the IL-11 pathway to inhibit PDCoV replication.

## The treatment of IL-11 inhibits the phosphorylation of the ERK signaling pathway

In the classic signaling pathway of IL-11, the JAK/STAT signaling pathway is the most well-established downstream pathway (31, 32). Previous studies have reported that IL-11 can inhibit the replication of PEDV, another porcine enteric coronavirus, by activating the IL-11/IL-11R/STAT3 signaling pathway (25). To further investigate the signaling pathway through which IL-11 exerts its antiviral effect on PDCoV replication, we treated IPI-2I cells with different doses (0, 10, 100, and 500 µg/mL) of recombinant IL-11 protein, followed by infection with PDCoV at an MOI of 1 for 24 h. Through Western blotting, we examined the expression and phosphorylation levels of signaling pathway proteins, including STAT3, AKT1, and ERK. As shown in Fig. 7A through F, only the phosphorylation level of ERK1/2 was suppressed by IL-11 treatment, and this inhibitory effect displayed a

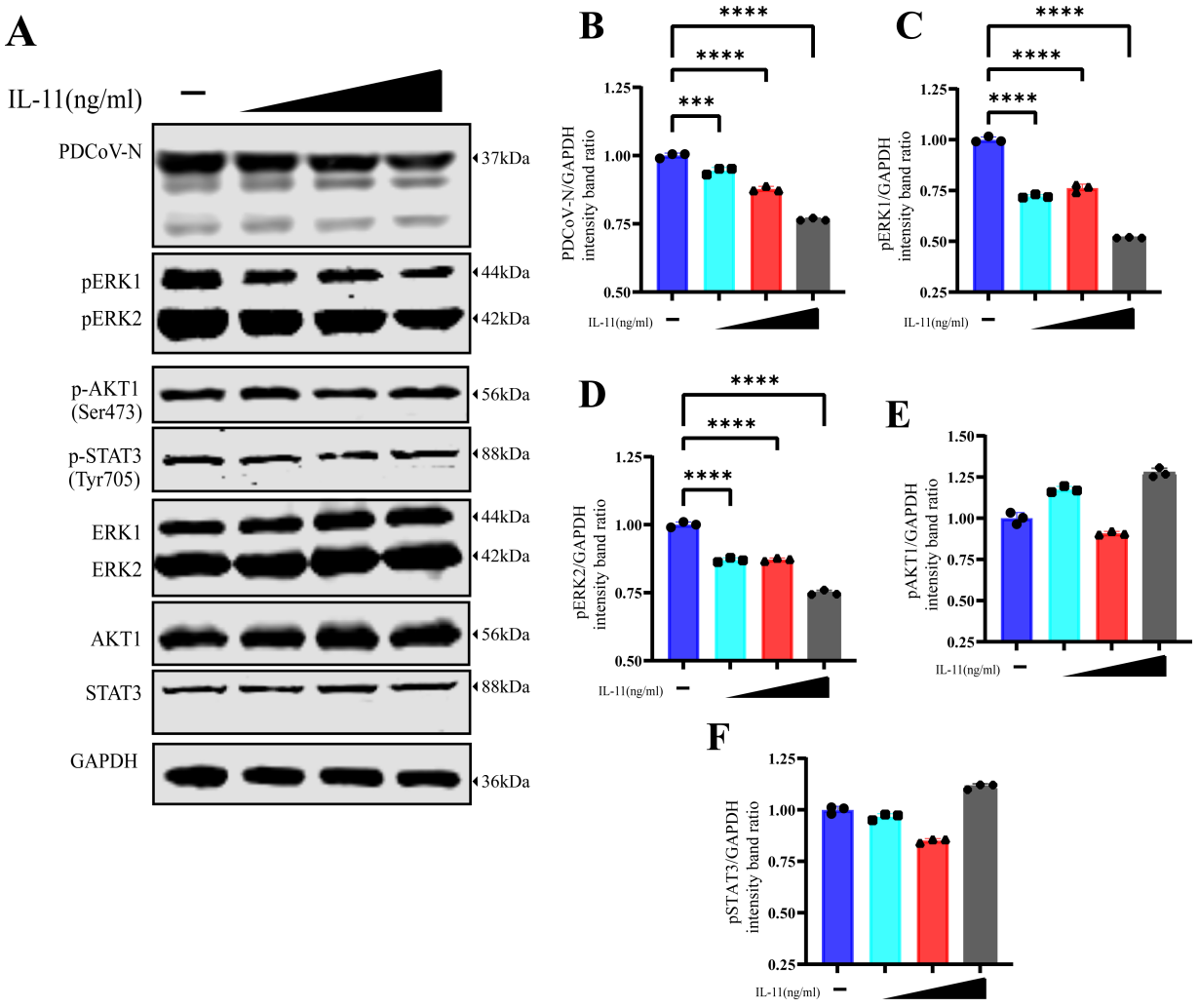


**FIG 7** The treatment of IL-11 inhibits the phosphorylation of the ERK signaling pathway. After infection with PDCoV at an MOI of 1, IPI-2I cells were treated with different doses (0, 10, 100, and 500) µg/mL of recombinant IL-11 protein. (A) The total proteins and phosphorylation proteins' expression of ERK1, ERK2, AKT1, and STAT3 were measured by Western blotting. (B–F) The relative intensities of PDCoV-N (B), pERK1 (C), pERK2 (D), pAKT1 (E), and pSTAT3 (F) were normalized to that of glyceraldehyde-3-phosphate dehydrogenase (GAPDH). The means and SD of the results from three independent experiments are shown. ***$P < 0.001$ and ****$P < 0.0001$.

dose-dependent manner. Therefore, we concluded that exogenous treatment with IL-11 significantly inhibits the phosphorylation of the ERK signaling pathway.

## Inhibiting ERK phosphorylation hinders PDCoV replication

ERK1/2, a member of the MAPK cascade pathway, plays a crucial role in regulating various cellular processes, including proliferation, differentiation, survival, and apoptosis (33–35). Swine acute diarrhea syndrome coronavirus (SADS-CoV) replication is reduced by inhibition of the ERK signaling pathway (36). To evaluate the effect of inhibiting ERK phosphorylation on PDCoV replication, the ERK signaling pathway inhibitor U0126 was used. First, the CCK-8 cell viability assay was used to investigate the impact of U0126 on the viability of IPI-2I cells at different concentrations. As shown in Fig. 8A, there was no significant difference in cell viability between the treatment group and the control group when the inhibitor concentration ranged from 0 to 200 µM. To further validate the effect of the ERK signaling pathway on PDCoV replication, we treated IPI-2I cells with U0126 at concentrations of 5, 10, 20, 50, and 100 µM, respectively, followed by infection with PDCoV at an MOI of 1. Cell samples were collected for RT-qPCR and Western blotting at 24 hpi, and the supernatant was collected for $TCID_{50}$ assay to determine the virus titer. As shown in Fig. 8B, the phosphorylation of ERK1/2 was significantly inhibited by U0126, and the replication of PDCoV was inhibited in a dose-dependent manner by U0126. The $TCID_{50}$ assay results (Fig. 8C) showed consistent results in the virus titer of the collected supernatant. Thus, inhibiting the phosphorylation of the ERK signaling pathway significantly reduced the intracellular replication of PDCoV. Taken together, these results indicated that NLRP1 suppresses the phosphorylation of ERK protein by upregulating IL-11 expression, thereby inhibiting intracellular PDCoV replication and exerting its antiviral effect.

The efficacy of U0126 in inhibiting other porcine enterocoronaviruses is well-established, such as PEDV and SADS-CoV (36, 37). Therefore, we also explored whether U0126 has antiviral effects on TGEV, and the results showed that the ERK phosphorylation inhibitor U0126 effectively hindered TGEV replication (Fig. 8D and E). These results indicate that U0126 has therapeutic potential against porcine enterocoronavirus.

## Inhibition of the phosphorylation of the ERK signaling pathway suppresses PDCoV infection in piglets

To further verify whether ERK1 phosphorylation inhibitor-U0126 can exert antiviral effects in pigs, specific pathogen-free (SPF) piglets were infected with PDCoV and animals were treated once daily with 15 mg/kg U0126, starting on the day of infection. Severe diarrhea began at 36 h post-infection in the PDCoV infection group, and at 72 hpi, all surviving piglets were euthanized to reduce the stress of the other piglets. Virus loads in fecal swabs at different time points of artificially infected piglets were tested by the RT-qPCR. The results showed that the viral load in fecal swabs of the PDCoV-infected group was the highest at 36 hpi. The viral load in the fecal swabs of U0126-treated piglets was significantly lower than that in the PDCoV-infected group and was barely detectable after 48 hpi (Fig. 9A).

The small intestinal wall became thin, which was especially true for the jejunum, and animals presented with intestinal dilation with an abundance of yellow liquid. In the U0126-treated group, the small intestinal wall was slightly thinner than that in the mock group. Overall, the damage to the small intestine in the PDCoV group was significantly worse than that in the U0126-treated group (Fig. 9B). Moreover, hematoxylin and eosin (H and E) staining revealed extensive fine damage to the jejunum, characterized by the fragmentation and shedding of intestinal villi (Fig. 9C). Next, we analyzed the viral infection efficiency in the intestine. The results showed that treatment of piglets with U0126 resulted in significant inhibition of PDCoV replication in the intestine (Fig. 9D). Immunohistochemistry showed that the virus was present in the PDCoV-infected group but not in the U0126-treated group, consistent with the clinical results (Fig. 9E).

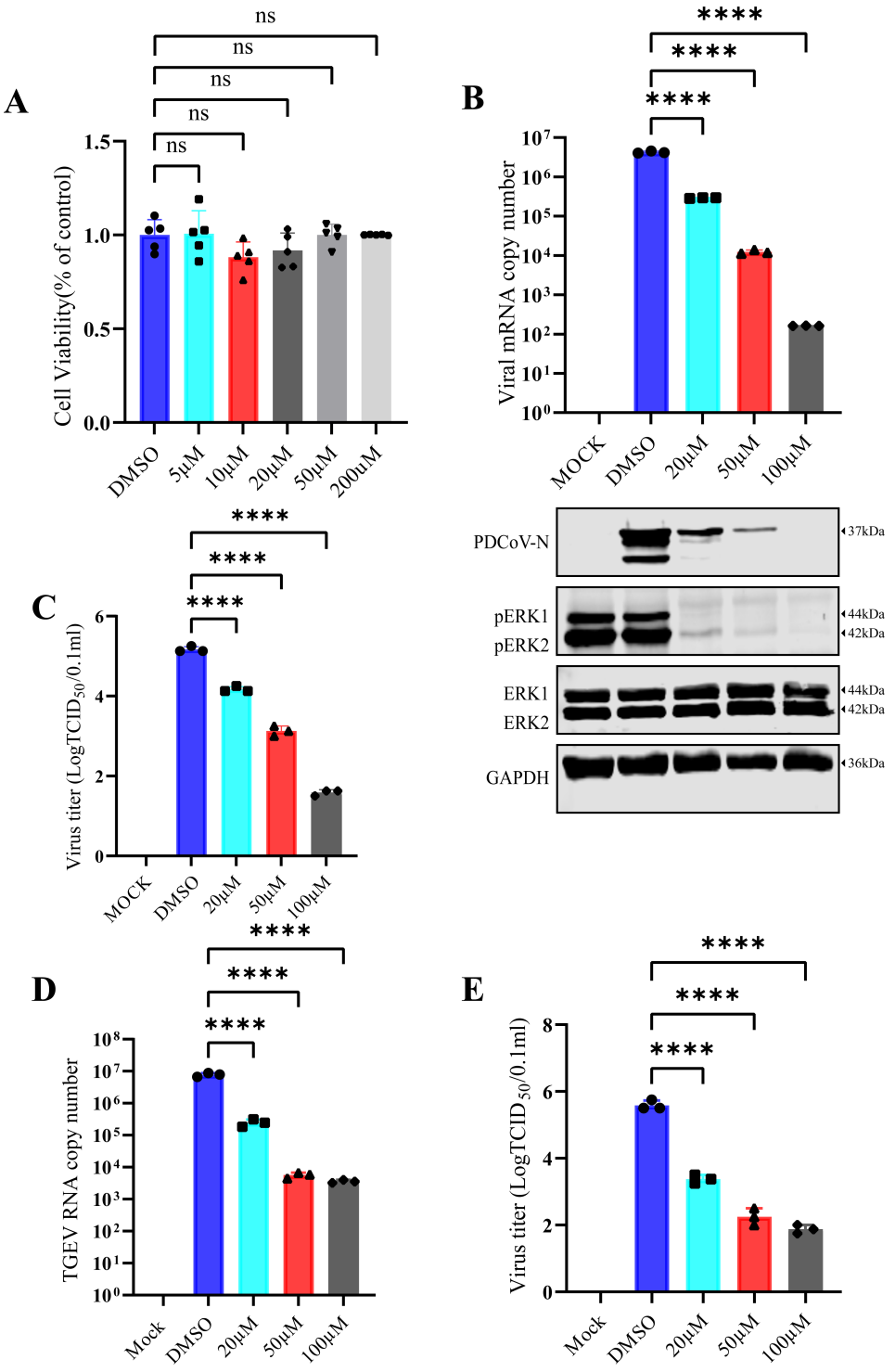


**FIG 8** The phosphorylation inhibitor of ERK1/2 (U0126) significantly inhibits the replication of PDCoV in cells. (A) Cell viability of IPI-2I treated with different concentrations (0, 5, 10, 20, 50, and 200 µM) of U0126. (B) The viral copy number and the expression of PDCoV-N were tested by RT-qPCR and Western blotting in U0126-treated cells. (C) The PDCoV $TCID_{50}$ in the supernatants was titrated on swine testis (ST) cells. (D) IPI-2I cells were treated with different concentrations (0, 20, 50, and 100 µM) of U0126, followed by infection with TGEV at an MOI of 0.1 for 24 h. The viral copy number of TGEV was determined by RT-qPCR. (E) The TGEV $TCID_{50}$ in the supernatants was titrated on ST cells. The means and SD of the results from three independent experiments are shown. ns, no significant difference. ***$P < 0.001$ and ****$P < 0.0001$.

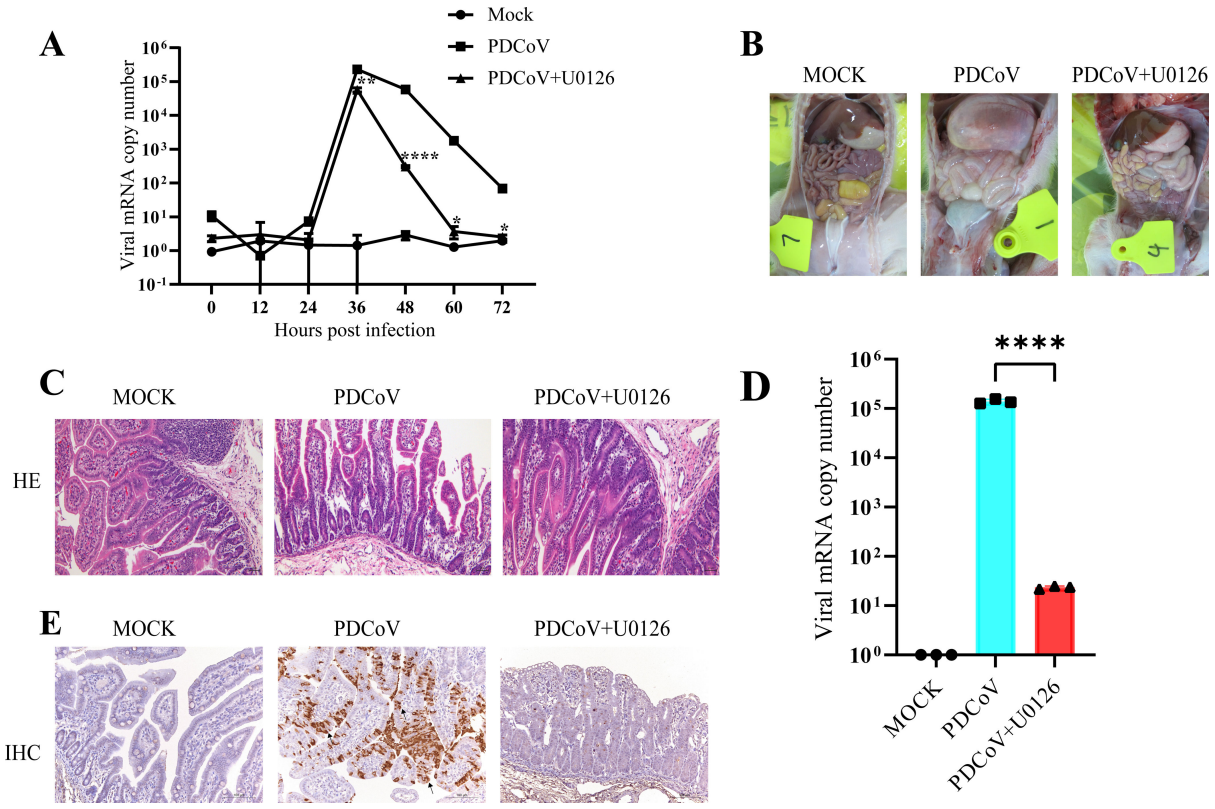


**FIG 9** U0126 suppresses PDCoV replication in piglets. SPF pigs were infected with PDCoV ($n$ = 3) or infected with PDCoV and treated with U0126 (15 mg kg$^{-1}$, $n$ = 3), or mock infected with Dulbecco's modified Eagle's medium ($n$ = 3). (A) Daily virus shedding in feces from the different groups was measured by RT-qPCR detection of viral genomes in fecal swabs. (B) Gross lesions in piglets inoculated with the PDCoV group or U0126-treated group. The intestinal lesions were examined on the day of death or after euthanasia at the final time points. The necropsy images show transparent intestines observed in piglets inoculated with the PDCoV group but not in mock-inoculated piglets. (C) Histopathological examination of the jejunum from the PDCoV-infected piglets. Jejunum was taken from each group and then processed for hematoxylin and eosin staining. Representative images are shown. (D) PDCoV viral RNA in the jejunum was measured by RT-qPCR. (E) Immunohistochemistry of jejunum from the piglets. The black arrows point to the virus in the tissue.

Taken together, these data confirmed that inhibition of the phosphorylation of the ERK signaling pathway suppresses PDCoV replication *in vivo*.

## DISCUSSION

NLRP1 can form an inflammasome complex that triggers cell pyroptosis and hinders pathogen replication by recognizing diverse PAMPs, such as double-stranded RNA and virus-encoded proteins (17, 19, 38). However, being the first-discovered inflammasome-forming protein, there has been limited research on the direct modulation of viral replication by the NLRP1 protein. Our early research revealed the function of NLRP1 as an ISG to resist TGEV infection (21). In this study, we present the inaugural evidence that NLRP1 inhibits PDCoV infection through the elevation of IL-11 expression, resulting in the suppression of ERK phosphorylation, rather than through the regulation of the IFN-I signaling pathway (Fig. 10).

NLRP6 binds viral RNA through the RNA helicase Dhx15 and interacts with MAVS, leading to the induction of type I/III IFNs and ISGs. This function plays a crucial role in the regulation of intestinal antiviral immunity. In contrast, our study revealed that overexpression of pNLRP1 following PDCoV infection had no impact on IFN-β production but significantly increased the expression of the cytokine IL-11. IL-11, a member of the IL-6 cytokine family, is secreted by a variety of cell types, including hepatocytes, gastrointestinal epithelial cells, T cells, B cells, and macrophages (39, 40). This cytokine is detectable in tissues associated with inflammation-related diseases and possesses

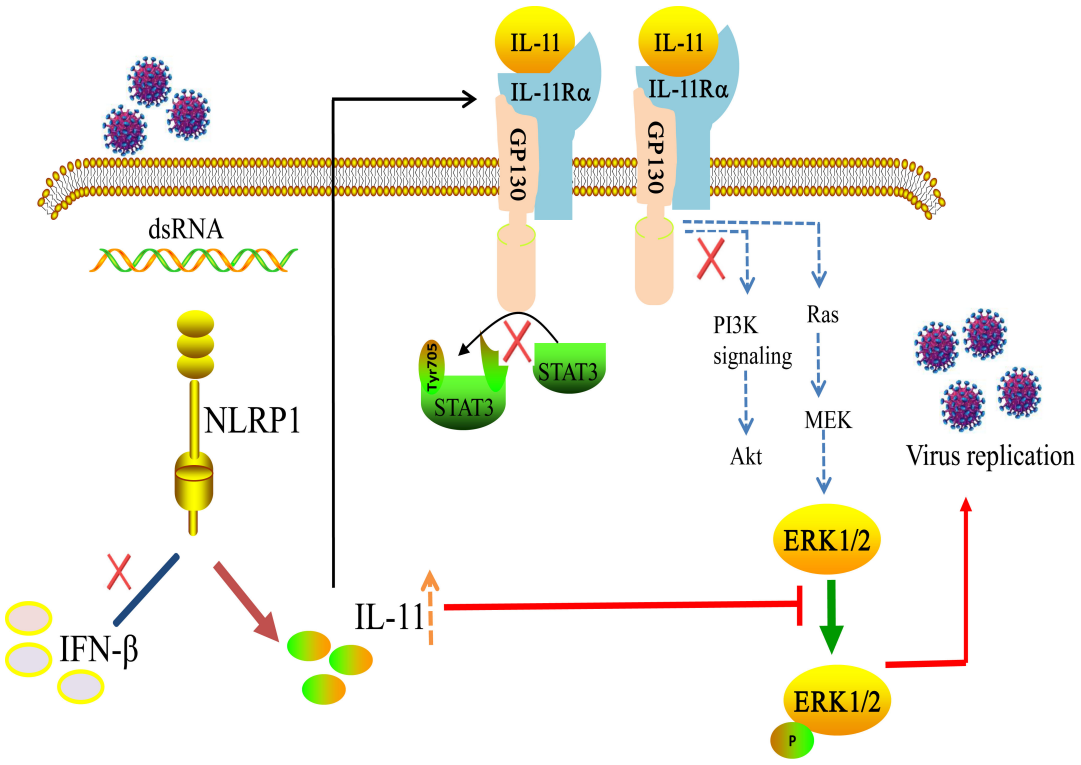


**FIG 10** The mechanism of NLRP1 inhibits PDCoV infection. NLRP1 suppressed the PDCoV replication by promoting the secretion of IL-11 to inhibit the phosphorylation of the ERK signaling pathway.

significant anti-inflammatory properties. Extensive research has been conducted on IL-11, particularly in the context of fibrotic diseases and solid malignancies, given its close association with their pathogenesis (23, 41, 42). Additionally, IL-11 demonstrates robust abilities in promoting the proliferation of intestinal cells and inhibiting apoptosis, providing significant protection against various injuries to intestinal epithelial cells (26–28, 43). Intestinal epithelial cells serve as target cells for porcine enteric coronaviruses, highlighting the potential significance of IL-11 in the context of virus invasion.

IL-11 engages the IL-11/STAT3 signaling pathway to impede PEDV-induced cell apoptosis, consequently suppressing viral infection (25). While the JAK/STAT signaling pathway has been extensively studied as a downstream pathway of IL-11, it is noteworthy that other signaling pathway proteins, such as ERK, MAPK, and PI3K/AKT, have also been reported to play roles in the regulation of IL-11 (23, 28). In this study, we examined several related signaling pathway proteins in IL-11-treated and PDCoV-infected cell samples. The results revealed a more pronounced inhibition of the ERK signaling pathway protein compared to STAT3 and AKT1, aligning with the suppression of viral replication (Fig. 7A). ERK1 and ERK2 belong to the MAPK family, a group of structurally related kinases. The ERK signaling pathway regulates six fundamental cellular processes: cell proliferation, survival, growth, metabolism, migration, and differentiation (44). Viruses, which depend on host cells for their survival, have evolved numerous strategies to exploit the ERK signaling pathway, enhancing their replication machinery for optimal infection. Recent studies have shown that ERK signaling is crucial for the efficient replication of several swine enteric coronaviruses, including PEDV, PDCoV, and SADS-CoV, in cultured cells (36, 37, 45). In our study, we observed a suppression of ERK phosphorylation in IPI-2I cells treated with various doses of IL-11 and infected with PDCoV. U0126 can reduce the titer of PDCoV progeny viruses in cell culture by more than 90%, which prompts us to speculate that U0126 may have high antiviral potential against PDCoV *in vivo*.

U0126 has been reported to have antiviral activity against pandemic H1N1 and highly pathogenic avian influenza virus *in vitro* and *in vivo* (46). Because of the obvious anti-PDCoV activity using U0126 *in vitro*, we additionally performed *in vivo* experiments using U0126 to investigate their antiviral potential in pigs. The results showed that U0126 has a high antiviral potential against PDCoV *in vivo*. U0126 has become commercially available, which is used in clinical trials against cancer. It has been demonstrated to cause a significant reduction in early liver tumor growth when administered intraperitoneally in mice and has shown promise in ameliorating post-stroke cerebral vasoconstriction in rats (47, 48). U0126 is not available in an oral formulation. As shown by Pinto and colleagues (49), intraperitoneal delivery of U0126 has an antiviral effect on influenza virus infection. For this reason, we decided to deliver U0126 intraperitoneally. Besides, U0126 also has an inhibition effect on TGEV replication (Fig. 8D and E). Our data demonstrate that ERK1 phosphorylation inhibitor might be very promising as a new class of antivirals against coronavirus.

Our results revealed an undiscovered mechanism employed by the host to resist coronavirus through the NLRP1-mediated regulation of the IL-11-ERK signaling pathway. The results clearly demonstrate the antiviral effectiveness of the ERK1 phosphorylation inhibitor in cell culture and in the piglets. This finding establishes a novel antiviral signal axis of NLRP1-IL-11-ERK, providing new insights into NLR-guided signal pathway and offering a promising therapeutic strategy for coronavirus infections.

## MATERIALS AND METHODS

### Cells and virus

IPI-2I cells, swine testis (ST) cells, Vero-E6 cells, and human embryonic kidney (HEK-293T) cells were cultured in Dulbecco's modified Eagle's medium (DMEM; Gibco, USA) supplemented with 10% fetal bovine serum (Gibco, USA) and maintained at 37°C in a 5% $CO_2$ humidified atmosphere. PDCoV strain NH10 (GenBank accession no. KU981062.1) and PDCoV strain NH100 (derived from strain NH10) were propagated and titrated in ST cells. TGEV strain H87, derived from the virulent strain H16 (GenBank accession no. FJ755618), was propagated and titrated in ST cells. PEDV strain CV777 (GenBank accession no. AF353511) was propagated and titrated in Vero-E6 cells.

### Viral infections and virus titration

For PDCoV infection, IPI-2I cells cultured in desired plates were infected with PDCoV at the indicated MOI or mock infected with DMEM. After incubation for 2 h at 37°C, cells were washed three times with phosphate-buffered saline (PBS) to remove unbound virus and cultured in maintenance medium (serum-free DMEM supplemented with 2.5 µg/mL trypsin) at 37°C for the indicated time points. The infected cell supernatants were harvested for testing virus titration. Briefly, ST cells were seeded into 96-well plates and cultured until 90% confluent. The infected cell supernatants were serially diluted 10-fold from $10^{-1}$ to $10^{-10}$. Next, ST cell monolayers were washed three times with PBS and then inoculated with dilutions. Cytopathic effects of the virus were observed after 72 h, and titers were calculated using the Reed and Muench method and expressed as $TCID_{50}$/0.1 mL.

### Antibodies

Rabbit polyclonal antibody (pAb) to AKT1, phospho-ERK1/2 rabbit monoclonal antibody (mAb), STAT3 rabbit mAb, phospho-STAT3-S727 rabbit mAb, and glyceraldehyde-3-phosphate dehydrogenase (GAPDH) rabbit mAb were purchased from Abcam (Cambridge, UK). Rabbit anti-NLRP1 pAb, phospho-AKT1-S473 rabbit mAb, and IL-11RA rabbit pAb were purchased from ABclonal (Wuhan, China). Mouse anti-FLAG M2 mAb and ERK1/2 rabbit pAb were purchased from Sigma (USA). Goat anti-rabbit and anti-mouse secondary antibodies conjugated to DyLight680, DyLight800, and goat anti-mouse

secondary antibody conjugated to peroxidase were purchased from Thermo Fisher Scientific (MA, USA). MAbs against PDCoV N protein were prepared and stocked by our team.

## RNA extraction and real-time quantitative PCR

Total RNA was extracted using a Simply P total RNA extraction kit (BioFlux, China) according to the manufacturer's protocol. The cDNA was synthesized from the purified RNA using a PrimeScript II first-strand cDNA synthesis kit (TaKaRa, Japan) according to the manufacturer's instructions. Real-time quantitative PCR was performed in triplicate on a QuantStudio5 system (Applied Biosystems, USA) with TB Green Premix Ex Taq II (Takara, Japan). All qPCR primer sequences are listed in Table 1. Relative gene expression levels were determined based on the cycle threshold ($^{\Delta\Delta}$CT) method and normalized to GAPDH expression.

## RNA interference

The siRNA targeting NLRP1, IL-11RA, and control scrambled were designed and purchased from Ribo (Guangzhou, China). All siRNA sequences are listed in Table 2. IPI-2I cells were seeded into 12-well plates for 16 h and then transfected with indicated siRNAs using Lipofectamine RNAiMAX reagent (Thermo Fisher Scientific, USA) following the manufacturer's protocol. Cells were infected with PDCoV at indicated MOI for 24 h at 24 h post-transfection. The siRNAs' knockdown efficiency of the target proteins was evaluated by RT-qPCR or Western blotting.

## Generation of NLRP1$^{-/-}$ cell lines

The NLRP1$^{-/-}$ cell line was generated in our laboratory as previously reported (21). Briefly, three guide RNAs were connected with the p × 330-U6-Chimeric_BB-CBh-hSpCas9 plasmid and then co-transfected with the pEGFP-C2 vector into IPI-2I cells. Two days later, GFP-positive cells were sorted into single clones on a 96-well plate by flow cytometry and then screened by RT-qPCR and Western blotting analysis.

## Cell viability assay

IPI-2I cells were seeded into 96-well plates for 24 h and then incubated with ERK inhibitor (U0126) at indicated concentrations or carrier control DMSO for 24 h. Cell viability was determined using the Cell Counting Kit-8 (CCK-8) assay (Dojindo, Japan) according to the

**TABLE 1** Sequences of RT-qPCR primers used in the study

| Primer | Sequence (5′–3′) |
|---|---|
| PDCoV-N-qPCR-F | AGCAACCACTCGTGTTACTTG |
| PDCoV-N-qPCR-R | CAACTCTGAAACCTTGAGCTG |
| IL-11-qPCR-F | ACTAAGCCTGTGGCCAGACAGAG |
| IL-11-qPCR-R | GATTACGATCTCCGTCAGCTGG |
| IL-11RA-qPCR-F | GTTCTGGAGCCAATACCGGA |
| IL-11RA-qPCR-R | GTGGGTCAGGGCGTAAGATG |
| IL-18-qPCR-F | GATAGCCTCACTAGAGGTCTG |
| IL-18-qPCR-R | GTATCTTATCATCATGTCCAGG |
| IL-1β-qPCR-F | GAAAGCCCAATTCAGGGACC |
| IL-1β-qPCR-R | TTCCTTGGCGGGTTCAGGTA |
| NLRP1-qPCR-F | ACAAGCTGCATGGACAGGTAC |
| NLRP1-qPCR-R | GATAGAGGCGGTCCTTACAGG |
| IFN-β-qPCR-F | AGCACTGGCTGGAATGAAAC |
| IFN-β-qPCR-R | TCCAGGATTGTCTCCAGGTC |
| GAPDH-qPCR-F | CCTTCCGTGTCCCTACTGCCAAC |
| GAPDH-qPCR-R | GACGCCTGCTTCACCACCTTCT |

**TABLE 2** Sequences of siRNAs used in the study

| Small interfering RNA | Sequence (5′–3′) |
|---|---|
| NC | TTCTCCGAACGTGTCACGT |
| siNLRP1#1 | CCAAGTTGCCCACTTCAAA |
| siNLRP1#2 | CCTCACCTTCACCCTCAAA |
| siIL-11RA#1 | AGAGTTCTGGAGCCAATAC |
| siIL-11RA#2 | GGAACCAGCAACACTCACA |

manufacturer's instructions. Briefly, 10 µL of CCK-8 solution was added to each well after treatment. The plates were incubated at 37°C for 2 h, and then the absorbance was read at a wavelength of 450 nm.

## Chemical treatment

Recombinant human IL-11 protein was purchased from ABclonal (Wuhan, China). After incubation with indicated MOI of PDCoV for 2 h at 37°C, IPI-2I cells were washed three times with PBS to remove unbound virus and then treated with different concentrations of IL-11 protein (0, 10, 100, or 1,000 ng/mL) for the indicated time points. ERK inhibitor (U0126) was purchased from Beyotime (Shanghai, China). IPI-2I cells were pretreated with various concentrations of U0126 (20, 50, and 100 µM) or with the same volume of DMSO, followed by infection with PDCoV at an MOI of 1. After incubation for 2 h, the supernatant was removed and replaced with a maintenance medium containing various doses of U0126. Cells were collected at 24 hpi and then the desired protein expression was detected by Western blotting and RT-qPCR.

## Plasmid construction and transfection

The cDNA of pNLRP1 was amplified from the porcine alveolar macrophage passage cell lines as described previously (21). Briefly, the full-length of pNLRP1 was cloned into the p3 × FLAG-CMV-10 vector by homologous recombination using the ClonExpress Ultra One Step Cloning Kit (Vazyme, China). All primer sequences are listed in Table 3. Plasmids were transfected into IPI-2I cells using Lipofectamine 3000 transfection reagent (ThermoFisher, USA), following the manufacturer's instructions. For HEK-293T cells, X-tremeGENE HP reagent (Roche, Switzerland) was used as the transfection reagent.

## Western blotting

All cell samples were collected to detect the indicated protein expression after plasmid transfection or PDCoV infection. Cells were harvested in 100 µL RIPA buffer (Beyotime, China) supplemented with 1 mM PMSF Solution (Beyotime, China) for 20 min on ice. The supernatant was separated by centrifugation at 14,000 rpm for 10 min at 4°C and boiled with 5× SDS-PAGE Sample Loading Buffer (Beyotime, China) for 10 min. Cell lysates were electrophoresed on 12.5% sodium dodecyl sulfate-polyacrylamide gel electrophoresis and electroblotted onto nitrocellulose filter membranes (Pall, USA) in transfer buffer (0.5 mM Tris-HCl, 20% methanol, and 0.2 M glycine). The membrane was blocked with 5% (wt/vol) skimmed milk for 2 h at room temperature and incubated with the primary antibodies at 4°C overnight. Subsequently, the membranes were incubated with DyLight680 or DyLight800 for 1 h at room temperature before washing three times with PBST. Finally, after being washed three times with PBST, immunolabeled proteins were scanned in an Odyssey Infrared Imaging System (LiCor BioSciences, USA). Quantification of band intensities by densitometry was performed using the Image J software.

**TABLE 3** Sequences of primers used to construct the plasmids in the study

| Primer | Sequence (5′–3′) |
|---|---|
| NLRP1-F | TTGCGGCCGCGAATTCAATGAGTCTCACTGAATTAATCATAAAAGCCTCG |
| NLRP1-R | ATGCCACCCGGGATCCTCAGAGCAGGTGTTCAGACAGC |

## PDCoV infection of piglets

Nine 1-day-old specific pathogen-free piglets were randomly divided into three groups and fed with fresh liquid milk diluted in warm water every 2 h. All piglets were confirmed to be free of PDCoV, TGEV, PEDV, and rotavirus by RT-PCR analysis of piglet feces before viral challenge. The piglet challenge group was inoculated orally with PDCoV at a dose of $1 \times 10^6$ $TCID_{50}$. For the compound administration group, U0126 was dissolved in 10% DMSO, 40% PEG300 (Sigma), 5% Tween-80, and 45% PBS. U0126 was administered by intraperitoneal injection at 15 mg/kg in a volume of 600 µL once a day. The control group received vehicle only. After viral infection, clinical signs were recorded on a daily basis. All piglets were euthanized at 72 hpi. At necropsy, piglet small intestine samples were collected for RT-qPCR analyses or fixed in 10% formalin for histopathological examination and stained with H and E.

## Immunohistochemistry

Intestinal tissue samples were initially fixed in 10% formalin, followed by deparaffinization in xylene and rehydration using a descending ethanol concentration series (100%, 95%, and 70%). Antigen retrieval was conducted in a citrate buffer solution (pH 7.4) at 121°C for 30 min. Subsequently, slides were blocked with 5% skim milk in PBS at room temperature for 30 min. Antigen detection utilized a mouse anti-PDCoV-N monoclonal antibody (diluted 1:100) developed in our laboratory. Following an overnight incubation at 4°C, slides were washed thrice with PBS and then incubated with a goat anti-mouse secondary antibody for 40 min at room temperature. Visualization was achieved using diaminobenzidine (Sigma-Aldrich, USA), followed by counterstaining with hematoxylin. Finally, slides were dehydrated, clarified in xylene, mounted with Entellan mounting medium (Sigma-Aldrich, USA), and assessed for positive immune reactivity using an optical microscope.

## H & E staining

Tissue samples fixed in formalin were processed as follows: they were serially dehydrated using 70%, 95%, and 100% ethanol, subsequently cleared in xylene, embedded in paraffin wax, and sectioned to a thickness of 4–6 µm. Following dewaxing in xylene and sequential rehydration with 100%, 95%, and 70% ethanol, ileum sections underwent staining with hematoxylin and eosin (Sigma-Aldrich) for histopathological assessment. The sections were then examined using a light microscope.

## ELISA

The protein level of IL-11 in cell culture supernatants was measured by the Human IL-11 ELISA Kit purchased from ABclonal (Wuhan, China) according to the manufacturer's instructions. The protein levels of IFN-β in cell culture supernatants were measured by the Porcine IFN-β ELISA Kit purchased from Bioswamp (Wuhan, China) according to the manufacturer's instructions.

## Statistical analyses

Analysis of experimental data, standard deviations calculations, and graph plotting from the results of three independent experiments were performed using the GraphPad Prism software (version 9.0). All statistical analyses were performed by one-way analysis of variance. Differences were considered significant if the *P*-value was $< 0.05$.

## ACKNOWLEDGMENTS

This work was supported by the National Key Research and Development Program of China (2021YFD1801103 to M.X.) and the Natural Science Foundation for Excellent Young Scholars of Heilongjiang Province (YQ2022C041 to M.X.).

## AUTHOR AFFILIATION

[1]State Key Laboratory for Animal Disease Control and Prevention, Harbin Veterinary Research Institute, Chinese Academy of Agricultural Sciences, Harbin, Heilongjiang, China

## AUTHOR ORCIDs

Haojie He http://orcid.org/0000-0002-2943-8730
Mei Xue http://orcid.org/0000-0001-5103-8525
Li Feng http://orcid.org/0000-0003-4123-0892

## FUNDING


| Funder | Grant(s) | Author(s) |
|---|---|---|
| MOST \| National Key Research and Development Program of China (NKPs) | 2021YFD1801103 | Mei Xue |
| Natural Science Foundation for Excellent Youth Scholars of Heilongjiang Province | YQ2022C041 | Mei Xue |


## AUTHOR CONTRIBUTIONS

Haojie He, Project administration, Writing – original draft | Yongfeng Li, Methodology, Validation, Writing – review and editing | Yunyan Chen, Validation | Jianfei Chen, Resources | Zhongyuan Li, Data curation, Validation | Liang Li, Methodology, Resources | Da Shi, Methodology, Resources | Xin Zhang, Resources | Hongyan Shi, Resources | Mei Xue, Funding acquisition, Methodology, Supervision, Writing – review and editing | Li Feng, Conceptualization, Resources, Supervision

## ETHICS APPROVAL

The PDCoV infection experiment was approved by the Animal Care and Ethics Committee of the Harbin Veterinary Research Institute.

## REFERENCES


1. Dong BQ, Liu W, Fan XH, Vijaykrishna D, Tang XC, Gao F, Li LF, Li GJ, Zhang JX, Yang LQ, Poon LLM, Zhang SY, Peiris JSM, Smith GJD, Chen H, Guan Y. 2007. Detection of a novel and highly divergent coronavirus from Asian leopard cats and Chinese ferret badgers in Southern China. J Virol 81:6920–6926. https://doi.org/10.1128/JVI.00299-07
2. Woo PCY, Lau SKP, Lam CSF, Lai KKY, Huang Y, Lee P, Luk GSM, Dyrting KC, Chan K-H, Yuen K-Y. 2009. Comparative analysis of complete genome sequences of three avian coronaviruses reveals a novel group 3c coronavirus. J Virol 83:908–917. https://doi.org/10.1128/JVI.01977-08
3. Woo PCY, Lau SKP, Lam CSF, Lau CCY, Tsang AKL, Lau JHN, Bai R, Teng JLL, Tsang CCC, Wang M, Zheng B-J, Chan K-H, Yuen K-Y. 2012. Discovery of seven novel mammalian and avian coronaviruses in the genus deltacoronavirus supports bat coronaviruses as the gene source of alphacoronavirus and betacoronavirus and avian coronaviruses as the gene source of gammacoronavirus and deltacoronavirus. J Virol 86:3995–4008. https://doi.org/10.1128/JVI.06540-11
4. Wang L, Byrum B, Zhang Y. 2014. Detection and genetic characterization of deltacoronavirus in pigs, Ohio, USA, 2014. Emerg Infect Dis 20:1227–1230. https://doi.org/10.3201/eid2007.140296
5. Ma Y, Zhang Y, Liang X, Lou F, Oglesbee M, Krakowka S, Li J. 2015. Origin, evolution, and virulence of porcine deltacoronaviruses in the United States. mBio 6:e00064. https://doi.org/10.1128/mBio.00064-15
6. He W-T, Ji X, He W, Dellicour S, Wang S, Li G, Zhang L, Gilbert M, Zhu H, Xing G, Veit M, Huang Z, Han G-Z, Huang Y, Suchard MA, Baele G, Lemey P, Su S. 2020. Genomic epidemiology, evolution, and transmission dynamics of porcine deltacoronavirus. Mol Biol Evol 37:2641–2654. https://doi.org/10.1093/molbev/msaa117
7. Dong N, Fang L, Yang H, Liu H, Du T, Fang P, Wang D, Chen H, Xiao S. 2016. Isolation, genomic characterization, and pathogenicity of a Chinese porcine deltacoronavirus strain CHN-HN-2014. Vet Microbiol 196:98–106. https://doi.org/10.1016/j.vetmic.2016.10.022
8. Jung K, Hu H, Eyerly B, Lu Z, Chepngeno J, Saif LJ. 2015. Pathogenicity of 2 porcine deltacoronavirus strains in gnotobiotic pigs. Emerg Infect Dis 21:650–654. https://doi.org/10.3201/eid2104.141859
9. Boley PA, Alhamo MA, Lossie G, Yadav KK, Vasquez-Lee M, Saif LJ, Kenney SP. 2020. Porcine deltacoronavirus infection and transmission in poultry, United States. Emerg Infect Dis 26:255–265. https://doi.org/10.3201/eid2602.190346
10. Jung K, Hu H, Saif LJ. 2017. Calves are susceptible to infection with the newly emerged porcine deltacoronavirus, but not with the swine enteric alphacoronavirus, porcine epidemic diarrhea virus. Arch Virol 162:2357–2362. https://doi.org/10.1007/s00705-017-3351-z
11. Liang Q, Zhang H, Li B, Ding Q, Wang Y, Gao W, Guo D, Wei Z, Hu H. 2019. Susceptibility of chickens to porcine deltacoronavirus infection. Viruses 11:573. https://doi.org/10.3390/v11060573
12. Liu Y, Wang B, Liang Q-Z, Shi F-S, Ji C-M, Yang X-L, Yang Y-L, Qin P, Chen R, Huang Y-W. 2021. Roles of two major domains of the porcine deltacoronavirus S1 subunit in receptor binding and neutralization. J Virol 95:e0111821. https://doi.org/10.1128/JVI.01118-21
13. Lednicky JA, Tagliamonte MS, White SK, Elbadry MA, Alam MM, Stephenson CJ, Bonny TS, Loeb JC, Telisma T, Chavannes S, Ostrov DA, Mavian C, Beau De Rochars VM, Salemi M, Morris JG. 2021. Independent infections of porcine deltacoronavirus among Haitian children. Nature 600:133–137. https://doi.org/10.1038/s41586-021-04111-z
14. Schroder K, Tschopp J. 2010. The inflammasomes. Cell 140:821–832. https://doi.org/10.1016/j.cell.2010.01.040
15. Sandstrom A, Mitchell PS, Goers L, Mu EW, Lesser CF, Vance RE. 2019. Functional degradation: a mechanism of NLRP1 inflammasome

activation by diverse pathogen enzymes. Science 364:eaau1330. https://doi.org/10.1126/science.aau1330
16. Tsu BV, Beierschmitt C, Ryan AP, Agarwal R, Mitchell PS, Daugherty MD. 2021. Diverse viral proteases activate the NLRP1 inflammasome. Elife 10:e60609. https://doi.org/10.7554/eLife.60609
17. Planès R, Pinilla M, Santoni K, Hessel A, Passemar C, Lay K, Paillette P, Valadão A-LC, Robinson KS, Bastard P, et al. 2022. Human NLRP1 is a sensor of pathogenic coronavirus 3CL proteases in lung epithelial cells. Mol Cell 82:2385–2400. https://doi.org/10.1016/j.molcel.2022.04.033
18. Yang X, Zhou J, Liu C, Qu Y, Wang W, Xiao MZX, Zhu F, Liu Z, Liang Q. 2022. KSHV-encoded ORF45 activates human NLRP1 inflammasome. Nat Immunol 23:916–926. https://doi.org/10.1038/s41590-022-01199-x
19. Bauernfried S, Scherr MJ, Pichlmair A, Duderstadt KE, Hornung V. 2021. Human NLRP1 is a sensor for double-stranded RNA. Science 371:eabd0811. https://doi.org/10.1126/science.abd0811
20. Broz P, Dixit VM. 2016. Inflammasomes: mechanism of assembly, regulation and signalling. Nat Rev Immunol 16:407–420. https://doi.org/10.1038/nri.2016.58
21. He H, Wang W, Li L, Zhang X, Shi H, Chen J, Shi D, Xue M, Feng L. 2023. Activation of the NLRP1 inflammasome and its role in transmissible gastroenteritis coronavirus infection. J Virol 97:e0058923. https://doi.org/10.1128/jvi.00589-23
22. Rose-John S. 2018. Interleukin-6 family cytokines. Cold Spring Harb Perspect Biol 10:a028415. https://doi.org/10.1101/cshperspect.a028415
23. Fung KY, Louis C, Metcalfe RD, Kosasih CC, Wicks IP, Griffin MDW, Putoczki TL. 2022. Emerging roles for IL-11 in inflammatory diseases. Cytokine 149:155750. https://doi.org/10.1016/j.cyto.2021.155750
24. Kortekaas RK, Burgess JK, van Orsoy R, Lamb D, Webster M, Gosens R. 2021. Therapeutic targeting of IL-11 for chronic lung disease. Trends Pharmacol Sci 42:354–366. https://doi.org/10.1016/j.tips.2021.01.007
25. Li Y, Wu Q, Jin Y, Yang Q. 2019. Antiviral activity of interleukin-11 as a response to porcine epidemic diarrhea virus infection. Vet Res 50:111. https://doi.org/10.1186/s13567-019-0729-9
26. Peterson RL, Wang L, Albert L, Keith JC, Dorner AJ. 1998. Molecular effects of recombinant human interleukin-11 in the HLA-B27 rat model of inflammatory bowel disease. Lab Invest 78:1503–1512.
27. Uemura T, Nakayama T, Kusaba T, Yakata Y, Yamazumi K, Matsuu-Matsuyama M, Shichijo K, Sekine I. 2007. The protective effect of interleukin-11 on the cell death induced by X-ray irradiation in cultured intestinal epithelial cell. J Radiat Res 48:171–177. https://doi.org/10.1269/jrr.06047
28. Yang L, Wang R, Gao Y, Xu X, Fu K, Wang S, Li Y, Peng R. 2014. The protective role of interleukin-11 against neutron radiation injury in mouse intestines via MEK/ERK and Pi3K/Akt dependent pathways. Dig Dis Sci 59:1406–1414. https://doi.org/10.1007/s10620-013-3015-0
29. Wang P, Zhu S, Yang L, Cui S, Pan W, Jackson R, Zheng Y, Rongvaux A, Sun Q, Yang G, Gao S, Lin R, You F, Flavell R, Fikrig E. 2015. NLRP6 regulates intestinal antiviral innate immunity. Science 350:826–830. https://doi.org/10.1126/science.aab3145
30. Yin L, Chen J, Li L, Guo S, Xue M, Zhang J, Liu X, Feng L, Liu P. 2020. Aminopeptidase N expression, not interferon responses, determines the intestinal segmental tropism of porcine deltacoronavirus. J Virol 94:e00480-20. https://doi.org/10.1128/JVI.00480-20
31. Mahboubi K, Biedermann BC, Carroll JM, Pober JS. 2000. IL-11 activates human endothelial cells to resist immune-mediated injury. J Immunol 164:3837–3846. https://doi.org/10.4049/jimmunol.164.7.3837
32. Thiem S, Pierce TP, Palmieri M, Putoczki TL, Buchert M, Preaudet A, Farid RO, Love C, Catimel B, Lei Z, Rozen S, Gopalakrishnan V, Schaper F, Hallek M, Boussioutas A, Tan P, Jarnicki A, Ernst M. 2013. mTORC1 inhibition restricts inflammation-associated gastrointestinal tumorigenesis in mice. J Clin Invest 123:767–781. https://doi.org/10.1172/JCI65086
33. Diehl N, Schaal H. 2013. Make yourself at home: viral hijacking of the PI3K/Akt signaling pathway. Viruses 5:3192–3212. https://doi.org/10.3390/v5123192
34. Ebisuya M, Kondoh K, Nishida E. 2005. The duration, magnitude and compartmentalization of ERK MAP kinase activity: mechanisms for providing signaling specificity. J Cell Sci 118:2997–3002. https://doi.org/10.1242/jcs.02505
35. Roux PP, Blenis J. 2004. ERK and p38 MAPK-activated protein kinases: a family of protein kinases with diverse biological functions. Microbiol Mol Biol Rev 68:320–344. https://doi.org/10.1128/MMBR.68.2.320-344.2004
36. Zhang J, Zhang L, Shi H, Feng S, Feng T, Chen J, Zhang X, Han Y, Liu J, Wang Y, Ji Z, Jing Z, Liu D, Shi D, Feng L. 2022. Swine acute diarrhea syndrome coronavirus replication is reduced by inhibition of the extracellular signal-regulated kinase (ERK) signaling pathway. Virology 565:96–105. https://doi.org/10.1016/j.virol.2021.10.009
37. Kim Y, Lee C. 2015. Extracellular signal-regulated kinase (ERK) activation is required for porcine epidemic diarrhea virus replication. Virology 484:181–193. https://doi.org/10.1016/j.virol.2015.06.007
38. Robinson KS, Teo DET, Tan KS, Toh GA, Ong HH, Lim CK, Lay K, Au BV, Lew TS, Chu JJH, Chow VTK, Wang DY, Zhong FL, Reversade B. 2020. Enteroviral 3C protease activates the human NLRP1 inflammasome in airway epithelia. Science 370:eaay2002. https://doi.org/10.1126/science.aay2002
39. Elias JA, Tang W, Horowitz MC. 1995. Cytokine and hormonal stimulation of human osteosarcoma interleukin-11 production. Endocrinology 136:489–498. https://doi.org/10.1210/endo.136.2.7835281
40. Paul SR, Bennett F, Calvetti JA, Kelleher K, Wood CR, O'Hara RM, Leary AC, Sibley B, Clark SC, Williams DA. 1990. Molecular cloning of a cDNA encoding interleukin 11, a stromal cell-derived lymphopoietic and hematopoietic cytokine. Proc Natl Acad Sci U S A 87:7512–7516. https://doi.org/10.1073/pnas.87.19.7512
41. Schafer S, Viswanathan S, Widjaja AA, Lim W-W, Moreno-Moral A, DeLaughter DM, Ng B, Patone G, Chow K, Khin E, et al. 2017. IL-11 is a crucial determinant of cardiovascular fibrosis. Nature 552:110–115. https://doi.org/10.1038/nature24676
42. Widjaja AA, Singh BK, Adami E, Viswanathan S, Dong J, D'Agostino GA, Ng B, Lim WW, Tan J, Paleja BS, Tripathi M, Lim SY, Shekeran SG, Chothani SP, Rabes A, Sombetzki M, Bruinstroop E, Min LP, Sinha RA, Albani S, Yen PM, Schafer S, Cook SA. 2019. Inhibiting interleukin 11 signaling reduces hepatocyte death and liver fibrosis, inflammation, and steatosis in mouse models of nonalcoholic steatohepatitis. Gastroenterology 157:777–792. https://doi.org/10.1053/j.gastro.2019.05.002
43. Frost BL, Jilling T, Caplan MS. 2008. The importance of pro-inflammatory signaling in neonatal necrotizing enterocolitis. Semin Perinatol 32:100–106. https://doi.org/10.1053/j.semperi.2008.01.001
44. Lavoie H, Gagnon J, Therrien M. 2020. ERK signalling: a master regulator of cell behaviour, life and fate. Nat Rev Mol Cell Biol 21:607–632. https://doi.org/10.1038/s41580-020-0255-7
45. Jeon JH, Lee YJ, Lee C. 2020. Porcine deltacoronavirus activates the Raf/MEK/ERK pathway to promote its replication. Virus Res 283:197961. https://doi.org/10.1016/j.virusres.2020.197961
46. Droebner K, Pleschka S, Ludwig S, Planz O. 2011. Antiviral activity of the MEK-inhibitor U0126 against pandemic H1N1V and highly pathogenic avian influenza virus *in vitro* and *in vivo*. Antiviral Res 92:195–203. https://doi.org/10.1016/j.antiviral.2011.08.002
47. Bessard A, Frémin C, Ezan F, Fautrel A, Gailhouste L, Baffet G. 2008. RNAi-mediated ERK2 knockdown inhibits growth of tumor cells *in vitro* and *in vivo*. Oncogene 27:5315–5325. https://doi.org/10.1038/onc.2008.163
48. Ahnstedt H, Mostajeran M, Blixt FW, Warfvinge K, Ansar S, Krause DN, Edvinsson L. 2015. U0126 attenuates cerebral vasoconstriction and improves long-term neurologic outcome after stroke in female rats. J Cereb Blood Flow Metab 35:454–460. https://doi.org/10.1038/jcbfm.2014.217
49. Pinto R, Herold S, Cakarova L, Hoegner K, Lohmeyer J, Planz O, Pleschka S. 2011. Inhibition of influenza virus-induced NF-kappaB and Raf/MEK/ERK activation can reduce both virus titers and cytokine expression simultaneously *in vitro* and *in vivo*. Antiviral Res 92:45–56. https://doi.org/10.1016/j.antiviral.2011.05.009